The Crystal and Molecular Structure of New Tetravalent Ruthenium Porphyrin. μ-Oxo-bis[(octaethylporphinato)ruthenium(IV) hydroxide]

Hideki Masuda,* Tooru Taga, Kenji Osaki, Hiroshi Sugimoto, Masayasu Mori, and Hisanobu Ogoshi*

Contribution from the Faculty of Pharmaceutical Sciences, Kyoto University, Shimoadachi-cho, Yoshida, Sakyo-Ku, Kyoto, Japan, the Faculty of Science, Osaka City University, Sugimoto-cho, Sumiyoshi-ku, Osaka, Japan, and the Department of Materials Science and Technology, Technologyical University of Nagaoka, Kamitomioka, Nagaoka, 949-54 Japan.
Received July 14, 1980

Abstract: The crystal structure of μ-oxo-bis[(octaethylporphinato)ruthenium(IV) hydroxide] has been determined by the X-ray method. The compound crystallizes in the tetragonal space group $P4/nnc$ with two oligometric molecules and two solvent methanols in a unit cell of dimensions $a = b = 13.98$ (1) Å and $c = 18.03$ (12) Å. The structure was solved by the heavy-atom method and refined to $R = 0.093$ for 882 reflection data. The oligometric molecule has crystallographical D_4—422 symmetry and contains the binuclear $(HO)N_4Ru–O–RuN_4(OH)$ coordination group with the bridging Ru–O distance of 1.847 (13) Å, the Ru–OH distance of 2.195 (26) Å, and the Ru–N distance of 2.067 (14) Å. The Ru–O–Ru* bond is explicitly linear, and the N–Ru–Ru*–N* torsion angle is 22.7°. The porphinato core is planar within 0.04 Å, and the tetravalent ruthenium ion lies approximately on the same plane. The staggered conformation is stabilized by the tetramolecular π–π interactions between the face-to-face contact porphyrins and by the dπ–pπ–dπ interaction in the Ru(IV)–O–Ru(IV) bond.

Tetravalent heme iron has been receiving much attention in connection with the oxidation process in catalase, horseradish peroxidase, and cytochrome *c* peroxidase.[1] Oxidative reaction of the native Fe(III) hemoprotein of peroxidase produces a tetravalent iron–porphyrin complex, compound II, as an intermediate complex.[2-4] The structure is considered to be strongly related to the catalytic function of the hemoprotein. This complex is, however, unstable in vivo and/or in vitro, and the materials of this complex or its analogous have never been obtained in a crystalline state. On the other hand, since ruthenium is a fifth-row transition metal in the homologous series with iron, the Ru ion has been considered as a suitable substitute for the Fe ion, in spite of the chemical differences between Ru and Fe atoms.[8a] So far four ruthenium(II)–porphyrin complexes have been studied by the X-ray method.[7] The title ruthenium(IV)–porphyrin complex was of interest as a substitute of the iron(IV) porphyrin as observed in compound II, and the structural details of this complex was expected to provide substantial geometric properties around the tetravalent metal ion.

A ruthenium(IV)–porphyrin complex was prepared by oxidation of (octaethylporphinato)carbonylruthenium, $Ru^{II}(OEP)(CO)$, with *tert*-butyl hydroperoxide in benzene solution,[5] but its magnetic susceptibility and optical spectra showed anomalous behaviors. The diamagnetic property contradicts the paramagnetic nature of the six-coordinate Ru(IV) ion, which is usually considered to have two unpaired electrons in the d_{xz} and d_{yz} orbitals and a pair of electrons in the d_{xy} orbital. The anomalous magnetic and optical data led to a $[Ru(OEP)(OH)]_2$ dimer or a $[Ru(OEP)(OH)]_2O$ oligomer as a possible composition. X-ray study provides the definite identification of this material as the latter, $[Ru(OEP)(OH)]_2O$. In this paper the structure of this μ-oxo oligometric molecule is described and it is compared with those of the other porphyrin oligomers and divalent ruthenium–porphyrin complexes reported to date.[7,13]

Experimental Section

A dark violet crystal suitable for X-ray study was grown by slowly evaporating a 10:1 mixed solvent of methylene chloride and methanol. Preliminary X-ray photographic examination led to tetragonal symmetry, and systematic absences of $hk0$ for $h + k$ odd, $0kl$ for $k + l$ odd, and hkl for l odd indicated the centrosymmetric space group $P4/nnc$. The crystal with dimensions $0.1 \times 0.2 \times 0.5$ mm^3 was mounted on a Rigaku AFC-5 diffractormeter using Mo Kα radiation ($\lambda_{K\alpha_1} = 0.70926$ Å) with a graphite monochrometer. The unit cell parameters refined by using the least-squares method on the 20 reflections whose angular settings were determined by using the automatic centering program are $a = b = 13.98$ (1) Å and $c = 18.03$ (12) Å. The calculated density, based on two $[Ru(OEP)(OH)]_2O$ and two methanol molecules per unit cell, is 1.27 g/cm^3 and agrees well with an observed density of 1.26 g/cm^3, as measured by flotation in aqueous calcium chloride solution. The linear absorption coefficient was 4.72 cm^{-1} for the Mo Kα radiation. Intensity data of the 1845 reflections in the range $2\theta < 50°$ were collected by the ω–2θ scanning technique. The scanning rate of 5° in ω per minute was used. During the course of data collection, three standards were measured every 60 reflections. The data were automatically converted to the F_o data in the usual manner. The standard deviation, $\sigma(F_o)$, was given by eq 1, where I_{pk} is the peak height, B_1 and B_2 are the low and high ω

$$\sigma(F_o) = \frac{F_o}{2I_o}\left(I_{pk} + \frac{t_{pk}}{t_B}(B_1 + B_2)\right)^{1/2} \quad (1)$$

backgrounds, respectively, measured on either side of the peak, and t_{pk}

* Address correspondence as follows: H.M., Kyoto University; H.O., Technical University of Nagaoka.

(1) (a) George, P. *Biochem. J.* **1953**, *55*, 220. (b) Brill, A. S. *Compr. Biochem.* **1966**, *14*, 447. (c) Iizuka, T.; Kotani, M.; Yonetani, T. *Biochim. Biophys. Acta* **1968**, *167*, 257. (d) Moss, T. H.; Ehrenberg, A.; Bearden, A. J. *Biochemistry* **1969**, *8*, 4159. (e) Lang, G. *Q. Rev. Biophys.* **1970**, *3*, 1.
(2) (a) Dunford, H. B.; Stillman, J. S. *Coord. Chem. Rev.* **1976**, *19*, 187. (b) Yonetani, T. *Adv. Enzymol. Relat. Areas Mol. Biol.* **1970**, *33*, 309. Yamasaki, I. In "Molecular Mechanisms of Oxygen Activation"; Hayaishi, O. Ed.; Academic Press: New York, 1974; p 535.
(3) (a) Yonetani, T.; Coulson, A. F. W. *Biochemistry* **1975**, *14*, 2389. (b) Yonetani, T.; Schleyer, H.; Ehrenberg, A. *J. Biol. Chem.* **1966**, *241*, 3240. (c) Yamada, H.; Yamasaki, I. *Arch. Biochem. Biophys.* **1974**, *165*, 728. (d) Jones, P.; Dunford, H. B. *J. Theor. Biol.* **1977**, *69*, 457.
(4) (a) Dolphin, D.; Forman, A.; Borg, D. C.; Fajer, J.; Felton, R. H. *Proc. Natl. Acad. Sci. U.S.A.* **1971**, *68*, 614. (b) Dolphin, D.; Muljiani, Z.; Rousseau, K.; Borg, D. C.; Fajer, J.; Felton, R. H. *Ann. N.Y. Acad. Sci.* **1973**, *206*, 177. (c) Felton, R. H.; Owen, G. S.; Dolphin, D.; Forman, A.; Borg, D. C.; Fajer, J. *Ibid.* **1973**, *206*, 504. (d) Dolphin, D.; Felton, R. H. *Acc. Chem. Res.* **1974**, *7*, 26. (e) Dolphin, D.; Niem, T.; Felton, R. H.; Fujita, S, *J. Am. Chem. Soc.* **1975**, *97*, 5288. (f) Johnson, E. G.; Niem, T.; Dolphin, D. *Can. J. Chem.* **1978**, *56*, 1381.
(5) Ogoshi, H.; Sugimoto, H.; Mori, M.; Yoshida, Z., submitted for publication.
(6) Ibers, J. A., Hamilton, W. C., Eds. "International Tables for X-ray Crystallography"; Kynoch Press: Birmingham, England, 1974; Vol. IV.
(7) (a) Cullen, D. L.; Meyer, E. F., Jr.; Srivastava, T. S.; Tsutsui, M. *J. Chem. Soc., Chem. Commun.* **1972**, *182*, 584. (b) Bonnet, J. J.; Eaton, S. S.; Eaton, G. R.; Holm, R. H.; Ibers, J. A. *J. Am. Chem. Soc.* **1973**, *95*, 2141. (c) Little, R. G.; Ibers, J. A. *Ibid.* **1973**, *95*, 8583. (d) Hopf, F. R.; O'Brien, T. P.; Scheidt, W. R.; Whitten, D. G. *Ibid.* **1975**, *97*, 277.

0002-7863/81/1503-2199$01.25/0

Table I. Positional and Thermal Parameters for the Atoms of $[Ru(OEP)(OH)]_2O \cdot CH_3OH$

atom	x^a	y	z	$\beta_{11}{}^b$	β_{22}	β_{33}	β_{12}	β_{13}	β_{23}
Ru	1/4	1/4	0.1476 (2)	30 (1)	30 (1)	34 (1)	0	0	0
O_1	1/4	1/4	0.0258 (12)	29 (6)	29 (6)	40 (8)	0	0	0
O_2	1/4	1/4	1/4	13 (9)	13 (8)	122 (28)	0	0	0
O(M)	1/4	1/4	−0.1946 (38)	164 (46)	164 (45)	42 (25)	0	0	0
C(M)	0.3316 (61)	1/4	−1/4	45 (35)	13 (10)	63 (40)	0	0	−1 (35)
N	0.3731 (10)	0.3319 (10)	0.1459 (9)	44 (8)	42 (8)	37 (5)	14 (7)	10 (7)	0 (7)
C_A	0.3780 (12)	0.4313 (11)	0.1460 (15)	34 (9)	24 (8)	68 (10)	−9 (7)	−3 (10)	−1 (9)
C_B	0.4778 (13)	0.4586 (14)	0.1474 (13)	31 (11)	39 (11)	61 (8)	−1 (9)	3 (10)	0 (10)
C_C	0.5296 (13)	0.3801 (15)	0.1493 (16)	32 (10)	52 (12)	85 (13)	−12 (9)	2 (12)	0 (13)
C_D	0.4635 (13)	0.2987 (17)	0.1456 (17)	28 (11)	45 (12)	53 (10)	−5 (9)	−7 (11)	−13 (11)
C_M	0.2991 (17)	0.4919 (14)	0.1483 (21)	42 (12)	22 (10)	87 (14)	9 (9)	13 (13)	−7 (11)
$C_{B\alpha}$	0.5126 (14)	0.5616 (13)	0.1477 (18)	40 (11)	38 (10)	95 (15)	−13 (8)	1 (12)	8 (12)
$C_{B\beta}$	0.5258 (19)	0.5989 (17)	0.0690 (19)	92 (20)	51 (15)	112 (18)	−20 (14)	6 (17)	11 (15)
$C_{C\alpha}$	0.6407 (18)	0.3711 (18)	0.1522 (28)	55 (16)	49 (14)	190 (31)	−20 (11)	32 (22)	−13 (23)
$C_{C\beta}$	0.6813 (26)	0.3631 (29)	0.0733 (24)	67 (24)	95 (29)	77 (20)	4 (22)	12 (20)	−4 (22)
$C_{C\beta'}$	0.6844 (74)	0.3773 (88)	0.2253 (50)	96 (75)	133 (90)	58 (50)	−4 (67)	−14 (48)	8 (54)

[a] Estimated standard deviations in the least significant figure(s) are given in parentheses. [b] The form of the anisotropic thermal parameter ellipsoid is $\exp[-(\beta_{11}h^2 + \beta_{22}k^2 + \beta_{33}l^2 + 2\beta_{12}hk + 2\beta_{13}hl + 2\beta_{23}kl)]$. The thermal parameters are multiplied by 10^4.

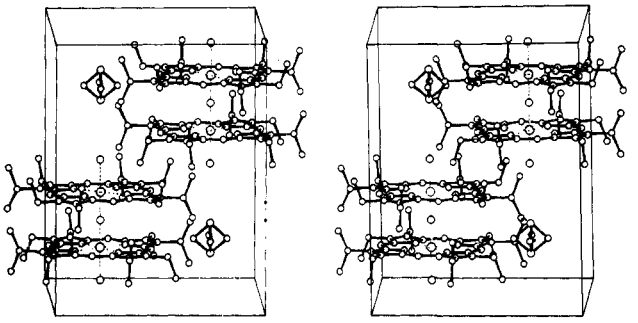

Figure 1. Stereoscopic view of the contents of one unit cell of $[(OEP)Ru(OH)]_2O \cdot CH_3OH$. The z axis is almost vertical, the y axis is horizontal to right, and the x axis is about perpendicular coming toward the reader. All the hydrogen atoms have been omitted.

and t_B are the measuring times of the peak and the background, respectively. A total number of 882 independent data for $F_o > 3\sigma(F_o)$ were considered as observed. The structure was solved by the heavy-atom method. The Ru atom was located by a sharpened Patterson synthesis, and the C, N, and O atoms of the $[Ru(OEP)(OH)]_2O$ oligomer were assigned by the successive Fourier synthesis. Subsequent refinement and difference Fourier synthesis revealed a disordered ethyl group and a solvent methanol molecule. The occupancy factors of these disordered atoms were estimated from the difference Fourier maps. The structure was refined by the full-matrix least-squares method. Atomic scattering factors and anomalous terms obtained from ref 6 were used. The function minimized was $\sum w(|F_o| - |F_c|)^2$ with $w = 1/(\sigma(F_o))^2$. Hydrogen atoms except for those of the disordered group were found in the difference Fourier maps and included in the structure factor calculation by assuming isotropic thermal parameters of 3.0 Å^2. The final values of the discrepancy indexes were 0.093 for $R = (\sum||F_o| - |F_c||/\sum|F_o|)$ and 0.1135 for $R_w = [\sum w(|F_o| - |F_c|)^2/\sum w(F_o)^2]^{1/2}$. All computations were performed on a FACOM M-190 in the Data Processing Center of Kyoto University, by using the program system KPAX.

Results and Discussion

The positional and anisotropic thermal parameters for all atoms except for the hydrogen atoms are listed in Table I. The crystal structure is stereographically depicted in Figure 1. The unit cell contains two $[Ru(OEP)(OH)]_2O$ and two methanol molecules. The two kinds of molecules are packed in a distorted NaCl type of arrangement with the van der Waals contacts. The binuclear oligomer exists at a crystallographical D_4—422 symmetry position. The required fourfold axis passes through the HO–Ru–O–Ru–OH bond, and the two twofold axes perpendicular to the fourfold axis pass through the central oxygen atom. Figure 2 displays a single $[Ru(OEP)(OH)]_2O$ molecule. One-fourth of the porphinato moiety is the asymmetric unit. The numbering scheme for the unique atoms is given in Figures 2 and 3. The disordered methanol molecule exists at another 422 symmetry position apart from the $[Ru(OEP)(OH)]_2O$ molecule by $z = {}^1/_2$. The oxygen atom occupies two sites with equal probability on the fourfold axis, and the carbon atoms occupies four sites on the twofold axes.

Bond lengths and angles for the porphyrin skeleton are given in Figure 3. Deviations from the least-squares plane of the 24 atoms on the porphinato core is also given on the left-hand side in Figure 3. The porphinato core is neither domed nor ruffled and is planar within 0.04 Å. The bond lengths and angles are quite normal in comparison with those reported for the planar porphyrins.[8]

Figure 4 presents a perspective diagram of the environment of one ruthenium ion. The ruthenium ion is displaced only by 0.03 Å out of the plane defined by the four porphinato nitrogen atoms. The Ru(IV)–N distance is 2.067 (14) Å. The Ru–N distance agrees well with the C_t–N distance, 2.062 Å, observed in metal-free OEP[11] and is slightly longer than the Ru(II)–N distances, 2.045–2.052 Å, reported in ruthenium(II)–porphyrin complexes.[12] This Ru–N distance indicates that the d_{xy} orbital of the Ru(IV) ion is fully occupied and the $d_{x^2-y^2}$ orbital is vacant. The Ru(IV)–O^{2-} distance is 1.847 (13) Å. This distance is comparable with the values reported for Ru(IV)–O^{2-}, 1.89 Å in inorganic RuO_2[19a,b] and 1.850 (4) Å in di-μ-oxo-bis(pentaammineruthenium)bis(ethylenediamine)ruthenium.[9] The longer Ru(IV)–O^{2-} distance compared with the Fe(III)–O^{2-} distance, 1.763 (1) Å, reported in μ-oxo-bis[(tetraphenylporphinato)iron(III)], $(TPPFe)_2O$,[13a] is consistent with the expected difference in the ionic radii of the Ru(IV) and Fe(III) ions.[10] The Ru(IV)–O(H) distance is 2.195 (26) Å. The Ru–O(H) distance is similar to the Ru(II)–OC_2H_5 distance, 2.21 (2) Å, in $TPPRu(CO)(OC_2H_5)$.[7b] However, it is considerably longer than the Ru(III)–O(H) distance, 1.98 Å, reported in $RuCl_2(OH)(NO) \cdot 4NH_3$[19c,d] and even longer than the sum of the ionic radii of the Ru(IV) and O atoms (2.02 Å).[10] The elongation of the Ru(IV)–O(H) bond may indicate that the hydroxide group is a very weakly bound ligand for the Ru(IV) ion.

Since the two ruthenium atoms in the μ-oxo dimer lie on the crystallographical fourfold axis, the Ru–O–Ru bond is explicitly

(8) (a) Hoard, J. L. "Porphyrins and Metalloporphyrins"; Smith, K. M., Ed.; Elsevier: Amsterdam, 1975; Chapter 8. (b) Hoard, J. L. *Science (Washington, D.C.)* **1971**, *174*, 1295. (c) Scheidt, W. R. *Acc. Chem. Res.* **1977**, *10*, 339.
(9) Smith, P. M.; Fealey, T.; Earley, J. E.; Silverton, J. V. *Inorg. Chem.* **1971**, *10*, 1943.
(10) Wells, A. F. "Structural Inorganic Chemistry"; Oxford University Press: New York, 1962.
(11) Lauher, J. W.; Ibers, J. A. *J. Am. Chem. Soc.* **1973**, *95*, 5148.
(12) Masuda, H.; Taga, T.; Osaki, K.; Sugimoto, H.; Yoshida, Z.; Ogoshi, H. *Inorg. Chem.* **1980**, *19*, 950.
(13) (a) Fleischer, E. B.; Srivastava, T. S. *J. Am. Chem. Soc.* **1969**, *91*, 2403. Hoffman, A. B.; Collins, D. M.; Day, V. W.; Fleischer, E. B.; Srivastava, T. S.; Hoard, J. L. *Ibid.* **1972**, *94*, 3620. (b) Scheidt, W. R.; Summerville, D. A.; Cohen, I. A. *Ibid.* **1976**, *98*, 6623. (c) Johnson, J. F.; Scheidt, W. R. *Ibid.* **1977**, *99*, 294.
(14) Fajer, J.; Borg, D. C.; Forman, A.; Dolphin, D.; Felton, R. H. *J. Am. Chem. Soc.* **1970**, *92*, 3451.

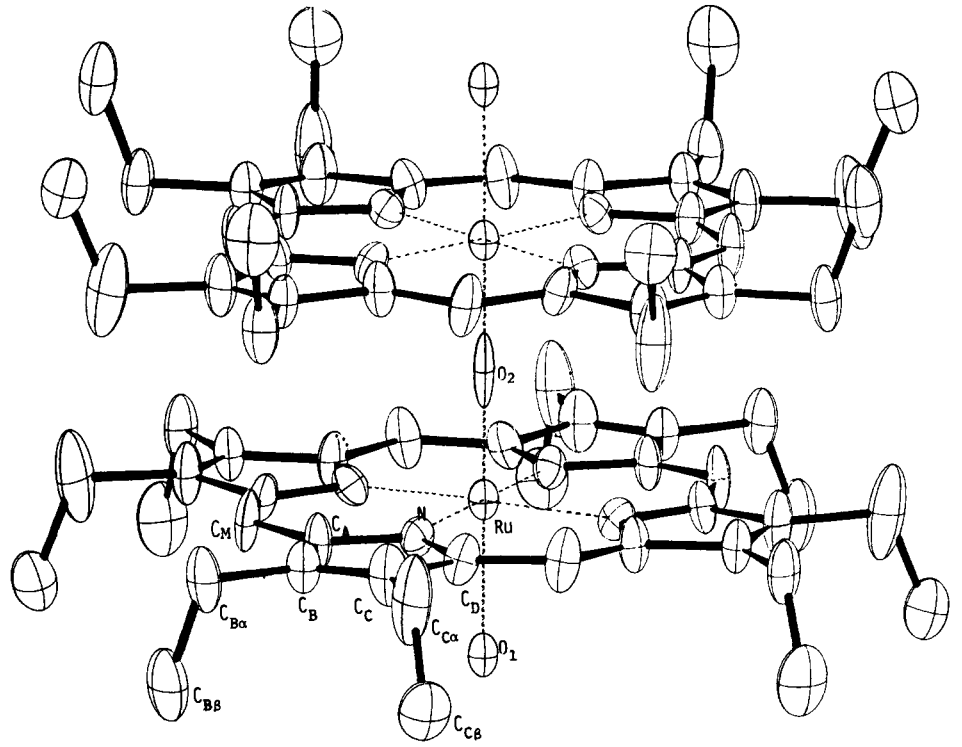

Figure 2. Computer-drawn model in perspective of the [(OEP)Ru(OH)]$_2$O molecule. The vibrational ellipsoids are drawn at the 30% probability level. The labeling scheme used for the atoms in the molecule is also shown.

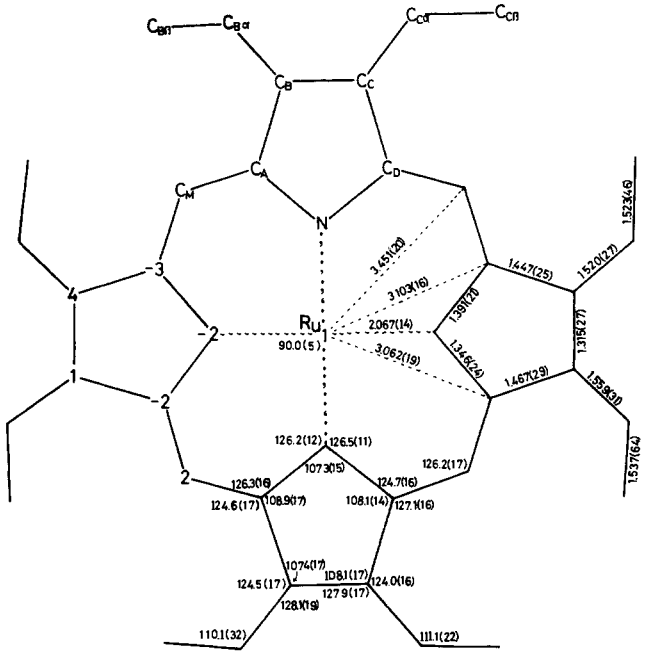

Figure 3. Formal diagram of the porphinato skeleton in [(OEP)Ru(OH)]$_2$O. On the top of the diagram, the numbering scheme for the atoms is displayed. On the left-hand side of the diagram, the numbered symbol for each atom is replaced by its perpendicular displacement, in units of 0.01 Å, from the mean plane of the porphinato core. On the right-hand side and the bottom of the diagram are the structurally independent atomic distances and bond angles. The bond distance and angle of the disordered ethyl group are 1.46 (11) Å for $C_{C\alpha}$–$C_{C\beta}'$ and 116 (5)° for C_C–$C_{C\alpha}$–$C_{C\beta}'$. The numbers in parentheses are the standard deviations of an individual distances or angles, as defined in Table I.

linear. The two porphinato cores related by the twofold symmetry are absolutely rotated about the straight Ru–O–Ru bond. The N–Ru–Ru*–N* torsion angle is 22.7°. The structure of the dimer is represented in terms of a "staggered conformation". The interplanar distance between the mean planes of the porphinato cores is 3.71 Å; the separations of each atom are 3.69 Å for Ru–Ru*, 3.84 Å for N–N*, 3.90 Å for C_A–C_A*, 3.72 Å for C_B–C_B*, and 3.74 Å for C_M–C_D*. The N–Ru–Ru*–N* torsion angle and the interplanar distances may be compared with the values of the corresponding angles and distances reported in the other μ-oxo and μ-nitrido porphyrin complexes, respectively: 35.4° and ~4.40 Å in μ-oxo-iron porphyrin;[13a] 31.7° and ~4.15 Å in μ-nitrido-iron porphyrin;[13b] 30° and ~3.8 Å in μ-oxo-molybdenum porphyrin.[13c] The small torsion angle compared with those of the other dimers may be related to the short interplanar distance, and the staggered structure will be interpreted by several intramolecular interactions, the steric hindrance between the peripheral groups, the π–π interactions between the face-to-face porphinato cores, and the μ-oxo-metal interactions. As shown in Figure 2, all terminal ethyl groups are oriented outside from the center of molecule except for that attached to C_C in the disordered state with 29% probability (torsion angles, C_A–C_B–$C_{B\alpha}$–$C_{B\beta}$ = −89.3°, C_C–C_B–$C_{B\alpha}$–$C_{B\beta}$ = 91.7°, C_B–C_C–$C_{C\alpha}$–$C_{C\beta}$ = −92.2°, C_D–C_C–$C_{C\alpha}$–$C_{C\beta}$ = 85.6°, C_B–C_C–$C_{C\alpha}$–$C_{C\beta}'$ = 84.6°, and C_D–C_C–$C_{C\alpha}$–$C_{C\beta}'$ = −97.7°). The peripheral ethyl groups do not prevent approach of the two porphinato cores and permit the direct core–core interaction (the large bulky phenyl groups at the meso positions of the other dimers[13] prevent their direct core–core interactions). The second π–π interactions between the face-to-face cores are possible enough within the observed interplanar distances. Even with a spacing of 6.0 Å, the existence of strong face-to-face interactions has been reported for the constrained *trans*-diurea binary iron(II) porphyrin[20a] and the *strati*-bisporphyrin.[20b] Thus, the interplanar distance less than 4 Å is sufficiently short for the π–π interaction. In fact, the π–π interaction is reflected in the anomalous absorption spectra in visible region, observed in CH_2Cl_2; absorption maxima are 377 (log ϵ_{max} = 5.30), 512 (4.12), and 580 nm (4.32) (Figure 7). The α band at 580 nm exhibits a bathochromic shift and large broadening in comparison with those of (OEP)$GeCl_2$ and (OEP)$SnCl_2$.[18] The π–π interaction is also rationalized from the viewpoint of the molecular orbital theory.[14] In the stacking diagram shown in Figure 5, approach between C_D and C_M* (C_M and C_D*) atoms favors the permissible charge transfer through the π–π* interaction from C_D (or C_D*) to C_M* (or C_M), and repulsion between C_A and C_A* atoms and between N and N* atoms is consistent with the repulsion between the localized

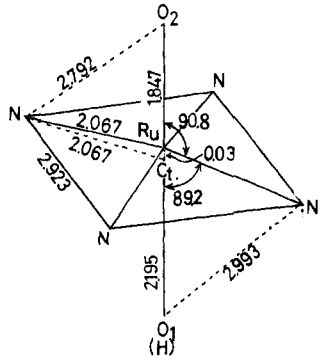

Figure 4. Perspective diagram of the six-coordination group around the ruthenium(IV) atom in the $[(OEP)Ru(OH)]_2O$ molecule. C_t represents the center of the porphine skeleton.

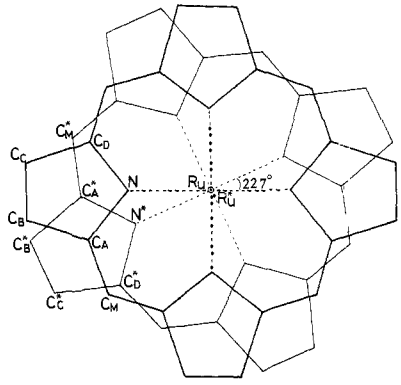

Figure 5. Stacking diagram of the two porphinato skeletons in the $[(OEP)Ru(OH)]_2O$ molecule approaching each other as viewed upright to the mean plane of the porphinato core atoms. The numbered symbols with an asterisk and those with no asterisk are in relation to the upper and lower core of the oligomeric porphyrin $[(OEP)Ru(OH)]_2O$.

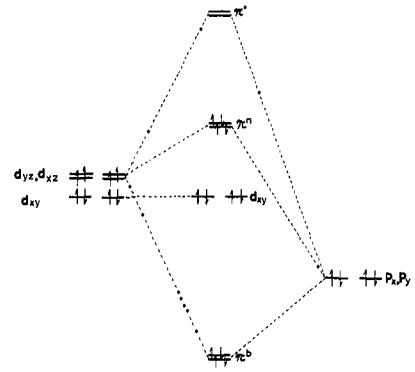

Figure 6. A qualitative MO scheme for the formation of the linear Ru–O–Ru system, showing π interactions between the two ruthenium atoms and bridging O.

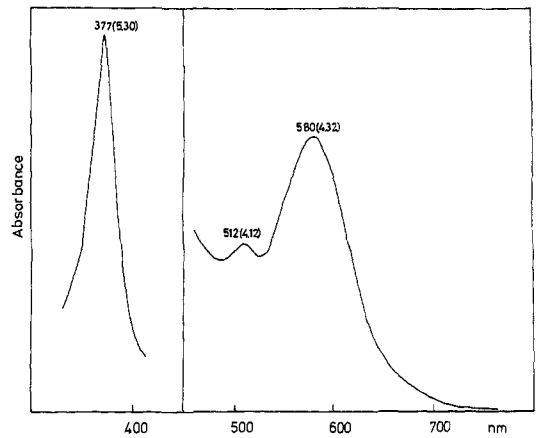

Figure 7. UV–visible spectrum for $[(OEP)Ru(OH)]_2O$ in CH_2Cl_2. Extinction coefficients (log ϵ_{max}) are given in parentheses following λ_{max} (nm).

electrons on these atoms. The ab initio MO calculation on porphinato core[15] shows that the N and C_M atoms have a large electron density distribution in the lowest unoccupied molecular orbital LUMO (E_g) and in the highest occupied molecular orbital HOMO (A_{2u}) and that the C_A and C_D atoms have a large electron density distribution in HOMO (A_{1u}). A similar example of the π–π* interaction has been observed in the $(OEP)FeClO_4$ complex,[12] although it is an intermolecular interaction. Existence of the third μ-oxo-metal interaction is evidenced by the diamagnetism of this complex (magnetic susceptibility = -899.65×10^{-6} cgs emu at 30.5 °C). According to the Dunitz and Orgel theory,[16] diamagnetism of a Ru(IV)–O–Ru(IV) system[17] has been explained by delocalization of the electrons in the Ru–O–Ru system. The short Ru(IV)–O bond compared with the sum of single-bond radii, 1.98 Å,[10] indicates considerably large double-bond character. In the linear Ru–O–Ru bond, the vacant d_{z^2} orbital of the Ru(IV) atom interacts with the bulky occupied sp-hybridized orbital of the oxo oxygen atom, and stable σ-bonding orbitals may be formed between the Ru and O atoms. The d_{xz} and d_{yz} unpaired electrons on the two Ru(IV) atoms fall into the bonding and nonbonding π orbitals formed by the $d\pi(Ru)$–$p\pi(O)$–$d\pi(Ru)$ interactions as shown in Figure 6. Absence of electrons on the π* level increases the stability of this system. The $d\pi$–$p\pi$–$d\pi$ interactions may be strictly related to the torsion angle about the Ru–O–Ru bond; the large interactions would be expected at N–Ru–Ru*–N* = 0. The d_{xz} and d_{yz} orbitals of the Ru atom also interact with the $p\pi$ orbitals of the weakly bound sixth ligand O(H). This $d\pi$-(Ru)–$p\pi$(OH) interaction was confirmed by the marked bathochromic shift of the α band (from 580 to 690 nm) by replacing the hydroxy anion with the more polarizable chloroanion.[5] This optical absorption band shift means that, in the allowed transition A_{1u}, A_{2u} of porphyrin → $d\pi$ (d_{xz}, d_{yz}) of metal, the $d\pi$ level is changed by the variation of the $d\pi$–$p\pi$ interaction.[21]

Conclusively, the short Ru–O^{2-} and Ru–N bonds clearly correspond to the vacant Ru(IV) d_{z^2} and $d_{x^2-y^2}$ orbitals, respectively, and the structural details of this complex are rationally consistent with the $S = 1$ spin state of the Ru(IV) atom with $(d_{xy})^2(d_{xz})(d_{yz})$ configuration, while the $S = 1$ spin state of the Fe(IV) atom has been reported, for compound II, on the basis of various spectroscopic studies.[3,4] The structural aspect around the Fe(IV) ion in compound II is expected to resemble that of the Ru(IV) ion, although the coordination about the Fe(IV) ion still is not obvious whether the axial ligands are imidazole and O^{2-} or imidazole anion and OH^-. For the undetermined axial ligand, the established structure provides the fact that the tetravalent metal ion has a

(15) (a) Case, D. A.; Karplus, M. *J. Am. Chem. Soc.* **1977**, *99*, 6182. (b) Gouterman, M. *J. Chem. Phys.* **1959**, *30*, 1139. (c) Spangler, D.; Maggiora, G. M.; Shipman, L. L.; Christoffeerson, R. E. *J. Am. Chem. Soc.* **1977**, *99*, 7478.

(16) Dunitz, J. D.; Orgel, L. E. *J. Chem. Soc.* **1953**, 2594.

(17) Mathieson, A. M.; Mellor, D. P.; Stephenson, N. C. *Acta Crystallogr.* **1952**, *5*, 185.

(18) Gouterman, M.; Schwarz, F. P.; Smith, P. D.; Dolphin, D. *J. Chem. Phys.* **1973**, *59*, 676.

(19) (a) Goldschmit, V. M. *Naturwissenschaften* **1926**, *14*, 477. (b) Lunde, G. *Z. Anorg. Chem.* **1927**, *163*, 345. (c) Bokii, G. B.; Parpiev, N. A. *Kristallografiya* **1957**, *2*, 691. (d) Parpiev, N. A.; Bokii, G. B. *Zh. Neorgan. Khim.* **1959**, *4*, 2452.

(20) (a) Collman, J. P.; Elliott, C. M.; Halbert, T. R.; Tovrog, B. S. *Proc. Natl. Acad. Sci. U.S.A.* **1977**, *74*, 18. (b) Kagan, N. E.; Mauzerall, D.; Merrifield, R. B. *J. Am. Chem. Soc.* **1977**, *99*, 5484.

(21) Antipas, A.; Buchler, J. W.; Gouterman, M.; Smith, P. D. *J. Am. Chem. Soc.* **1978**, *100*, 3015.

strong O^{2-} and a weak OH^- ligand in the axial direction and that the strong O^{2-} ligand is preferable to the $S = 1$ spin state of the central metal ion.

Acknowledgment. The authors wish to thank Professor Nobuo Morimoto and Dr. Katsutoshi Tomita, Faculty of Science in Kyoto University, for the use of the RIGAKU AFC-5 diffractometer.

Supplementary Material Available: A table of anisotropic thermal parameters and a listing of structure factor amplitudes (6 pages). Ordering information is given on any current masthead page.

Preparation and Thermal Decomposition of Pernitric Acid ($HOONO_2$) in Aqueous Media

Richard A. Kenley,* Paula L. Trevor, and Bosco Y. Lan

Contribution from SRI International, Menlo Park, California 94025. *Received August 11, 1980*

Abstract: Pernitric acid (PNA), $HOONO_2$, was prepared by reaction of HNO_3 or NO_2BF_4 with 90% H_2O_2 (either the neat liquid or in CH_3CN solution) at 273 K. Gaseous PNA was removed from the reaction mixtures with a stream of Ar and identified by its IR spectrum. Mass spectral data for PNA were obtained in a similar fashion. In aqueous buffer, PNA decomposes to give molecular oxygen and nitrite. This can be accounted for by the following reactions: $HOONO_2 \rightleftarrows H^+ + O_2NOO^-$ and $O_2NOO^- \rightarrow NO_2^- + O_2$. However, the possible intervention of radical reactions cannot be excluded. The observed first-order rate constant for oxygen evolution at 283.6 K and pH 4.7 is $(7.06 \pm 0.75) \times 10^{-3}$ s^{-1}.

Pernitric acid (PNA), $HOONO_2$, can be viewed either as an inorganic peracid, ROOH (where R = NO_2), a mixed anhydride of two acids (HOOH and HNO_3), or as the parent member of the family of peroxynitrates, $ROONO_2$ (where R = H). As such, PNA can be expected to participate in either free radical or ionic reactions, and it therefore affords the opportunity for some interesting kinetic and mechanistic investigations.

In 1911 D'Ans and Friederich[1] reacted H_2O_2 with N_2O_5 and obtained a solution that liberated Br_2 from Br^-. They suggested that the solution contained $HOONO_2$ but did not offer definitive proof for the existence of PNA. Schwarz[2] reported similar observations in 1948.

In 1977 Niki et al.[3] studied the gas-phase reaction of photochemically generated chlorine atoms with a mixture of H_2, O_2, and NO_2 and obtained the infrared spectrum of a species to which they assigned the formula HO_2NO_2. Other authors[4,5] have reported analogous photochemical methods for generating $HOONO_2$ in the gas phase. Graham et al.[6] condensed H_2O_2 in a 253-K trap and passed a mixture of 1% NO_2 in N_2 through the trap. They then degassed the trap under N_2 flow to yield PNA vapor.

The foregoing methods for generating $HOONO_2$ give a product that is contaminated with impurities and side products. As batch-type methods the existing procedures are not suitable for continuous generation of PNA such as might be required for gas-phase kinetic studies in flow systems. Moreover, the methods necessarily yield gaseous PNA, thereby precluding the possibility of investigating some interesting solution-phase chemistry.

It is well-known[7-10] that direct nitration of organic hydroperoxides yields peroxynitrates. The reaction can be generalized as in eq 1, where R = alkyl, acyl, and aroyl and X = OH, NO_3, or BF_4, etc. The original method of D'Ans and Friederich can be considered as an example of this basic process if the reagents are written in an appropriate fashion, i.e. as in eq 2. Nitric acid can also be written as $NO_2^+OH^-$ and nitryl fluoroborate as $NO_2^+BF_4^-$ by using this formalism.

$$ROOH + NO_2^+X^- \rightarrow ROONO_2 + HX \quad (1)$$

$$HOOH + NO_2^+NO_3^- (=N_2O_5) \rightarrow HOONO_2 + HNO_3 \quad (2)$$

In view of the foregoing we examined the potential utility of reaction 1 as a synthetic method for PNA. In this paper we describe the preparation of PNA in solution and the suitability of flow methods for generating relatively pure PNA vapor from the reaction mixtures. We also report on some decomposition reactions of $HOONO_2$.

Table I. Mass Spectral Data for Pernitric Acid (PNA), NO_2, and HNO_3

compd[a]	inlet temp, K	rel intens at m/e[b,c] 16	17	18	28	30	32	34	46
PNA	300	0.56	0.31	0.53	*d*	0.95	2.0	*d*	1
PNA	600	1.73	2.0	5.3	*d*	3.4	3.0	*d*	1
HNO_3	300	*e*	*e*	*e*	0.24	1.16	0.17	*e*	1
HNO_3	600	*e*	*e*	*e*	0.20	1.20	0.10	*e*	1
NO_2	600	*e*	*e*	*e*	0.10	4.1	*e*	*e*	1

[a] PNA prepared by mehod 2; see experimental details. HNO_3 prepared by reaction of H_2SO_4 with $NaNO_3$. [b] Each mass spectrum is separately normalized to m/e 46. [c] Relative intensity ≤0.05 for m/e not listed. [d] Relative intensity ≤0.20. [e] Relative intensity ≤0.05.

Results and Discussion

Preparation and Identification of PNA. We used three general procedures (see Experimental Section) for preparation of PNA at 273 K: (1) reaction of neat 90% H_2O_2 with 70% HNO_3; (2) reaction of neat 90% H_2O_2 with NO_2BF_4; (3) reaction of NO_2BF_4 and 90% H_2O_2 in CH_3CN.

Successful preparation of PNA was confirmed for methods 1 and 2 by warming the reaction mixtures to ambient temperature and passing a stream of Ar into the solutions and through a 10-cm path length IR cell or into a long path cell. In both cases, the characteristic IR spectrum of PNA[3,6] was readily observed.

On the basis of the reported value of the $HOONO_2$ absorption coefficient at 803 cm^{-1},[11] we calculate that concentrations of

(1) D'Ans, J.; Friederich, W. *Z. Anorg. Chem.* **1911**, *73*, 325.
(2) Schwarz, R. *Z. Anorg. Chem.* **1948**, *256*, 3.
(3) Niki, H.; Maker, P. D.; Savage, C. M.; Breitenbach, L. P. *Chem. Phys. Lett.* **1977**, *45*, 564.
(4) Hanst, P. L.; Gay, B. W. *Environ. Sci. Technol.* **1977**, *11*, 1105.
(5) Levine, S. Z.; Uselman, W. M.; Chan, W. H.; Calvert, J. G.; Shaw, J. H. *Chem. Phys. Lett.* **1977**, *48*, 528.
(6) Graham, R. A.; Winter, A. M.; Pitts, J. N. *Chem. Phys. Lett.* **1977**, *51*, 2–5.
(7) Hendry, D. G.; Kenley, R. A. In "Nitrogenous Air Pollutants, Chemical and Biological Implications"; Grosjean, D., Ed.; Ann Arbor Science: Ann Arbor, MI, 1979.
(8) Louw, R.; Sluis, G. J.; Vermeeren, H. P. W. *J. Am. Chem. Soc.* **1975**, *97*, 4396.
(9) Duynstee, E. F. J.; Housmans, J. G. H. M.; Vleugels, J.; Voskuil, W. *Tetrahedron Lett.* **1973**, *25*, 2275.
(10) Kenley, R. A.; Hendry, D. G. *J. Am. Chem. Soc.* **1977**, *99*, 3198.
(11) Graham, R. A.; Winer, A. M.; Pitts, J. N. *Geophys. Res. Lett.* **1978**, *5*, 909.

0002-7863/81/1503-2203$01.25/0